Journal of Solid State Chemistry **158,** 55–60 (2001)
doi:10.1006/jssc.2000.9056, available online at http://www.idealibrary.com

Investigations of the Copper Bromide–Ethylenediamine System: The Hydrothermal Synthesis and X-Ray Crystal Structure of $[Cu(H_2NCH_2CH_2NH_2)_2]\,[\{Cu_2Br_4\}]$ and $[Cu(H_2NCH_2CH_2NH_2)_2]\,[\{Cu_5Br_7\}]$

Robert P. Hammond,[1] Douglas J. Chesnut,[2] and Jon A. Zubieta[3]

Department of Chemistry, Syracuse University, Syracuse, New York, 13244

Received August 3, 2000; in revised form November 7, 2000; accepted December 8, 2000; published online March 8, 2001

The hydrothermal reactions of $CuBr_2$, CuBr, and ethylenediamine have resulted in the synthesis of two new compounds. $[Cu(H_2NCH_2CH_2NH_2)_2]\,[\{Cu_2Br_4\}]$ has a two-dimensional sheet structure while $[Cu(H_2NCH_2CH_2NH_2)_2]\,[\{Cu_5Br_7\}]$ crystallizes as a three-dimensional network. Both compounds were characterized by single-crystal X-ray diffraction. The following are the crystal data for $[Cu(H_2NCH_2CH_2NH_2)_2]\,[\{Cu_2Br_4\}]$ (1), triclinic space group $P1$ (No. 1) with $a = 6.491(1)$ Å, $b = 8.012(2)$ Å, $c = 8.070(2)$ Å, $\alpha = 107.713(5)^\circ$, $\beta = 109.976(4)^\circ$, $\gamma = 96.815(4)^\circ$, $Z = 1$, $d_{calc} = 2.88\ g\,cm^{-3}$, and $wR2\,(R1) = 0.093(0.037)$, and $[Cu(H_2NCH_2CH_2NH_2)_2]\,[\{Cu_5Br_7\}]$ (2), orthorhombic space group $Pnma$ (No. 62), with $a = 12.886(4)$ Å, $b = 16.776(5)$ Å, $c = 9.170(3)$ Å, $Z = 4$, $d_{calc} = 3.55\ g\,cm^{-3}$, and $wR2\,(R1) = 0.099$ (0.073). Both structures consist of anionic one-dimensional copper(I) bromide chains interspersed with cationic $[Cu(H_2NCH_2CH_2NH_2)_2]^{2+}$ units. © 2001 Academic Press

Key Words: **hydrothermal synthesis; X-ray crystal structure.**

INTRODUCTION

Solid state inorganic compounds not only are of significant fundamental interest but also have wide-ranging applications (1), yet their synthesis by rational design remains problematic. A powerful synthetic approach to the manipulation of the microstructures of solid state inorganic materials exploits the incorporation of organic components, which contribute to the increased complexity as one constituent in a hierarchical structure exhibiting a synergestic interaction between the organic and inorganic substructures (2, 3). Three primary classes of materials in which organic components play an important structural role have been studied extensively: zeolites (4), mesoporous oxides of the MCM-41 type (5), and biomineralized materials (6). More recently, we and others have expanded the organic/inorganic oxide materials to include two new families: the microporous transition metal phosphates with entrained organic cations (TMPOs) (7–11) and the organically templated vanadium and molybdenum oxides (12–24). This concept of templating anionic inorganic networks with organic constituents has also been extended to the metal halide and pseudohalide systems (25–31) in a demonstration of the wide-ranging applications of the general strategy.

The report of the hydrothermal synthesis of an anionic three-dimensional copper chloride framework with entrained $[Cu(H_2NCH_2CH_2NH_2)_2]^{2+}$ units (32) has prompted us to examine other copper halide systems for similar phases. As a part of that work, hydrothermal reactions of copper(I) and copper(II) bromide with ethylenediamine (hereafter abbreviated as *en*) have been investigated. This work represents a part of our efforts to extend this technique to metal halide systems. We report here the synthesis and structure determination of two compounds, $[Cu(en)_2]\,[\{Cu_2Br_4\}]$ and $[Cu(en)_2]\,[\{Cu_5Br_7\}]$.

EXPERIMENTAL SECTION

All syntheses were performed using reagent grade $CuBr_2$, CuBr, and ethylenediamine, purchased from the Aldrich Chemical Co., and used without further purification. All hydrothermal reactions were performed in 23-mL polytetrafluoroethylene-lined stainless steel Parr bombs under autogenous pressure.

$[Cu(H_2NCH_2CH_2NH_2)_2]\,[\{Cu_2Br_4\}]$, **1**. This phase was prepared by the reaction of $CuBr_2$ (0.670 g, 3.0 mmol) and ethylenediamine (0.20 mL; $d = 0.899\ g\,mL^{-1}$; 3.0 mmol) in 8 mL of H_2O in a mole ratio of 1 : 1 : 148 at 170°C for 3 days. A single-phase product consisting of dark

---

[1] Current address: Chalk River Laboratories, Chalk River, Ontario, Canada K0J 1J0.

[2] Current address: Department of Chemistry, Alfred University, Alfred, New York, 14802.

[3] To whom correspondence should be addressed.

0022-4596/01 $35.00

TABLE 1
Crystallographic Data and Structure Refinement for $[Cu(H_2NCH_2CH_2NH_2)_2][\{Cu_2Br_4\}]$ (1) and $[Cu(H_2NCH_2CH_2NH_2)_2][\{Cu_5Br_7\}]$ (2)

	Compound	
	1	**2**
Empirical formula	$Cu_3Br_4C_4H_{16}N_4$	$Cu_6Br_7C_4H_{16}N_4$
fw	630.47	1060.82
Space group	*P*1	*Pnma*
a (Å)	6.491(1)	12.886(4)
b (Å)	8.012(2)	16.776(5)
c (Å)	8.070(2)	9.170(3)
α (°)	107.713(5)	
β (°)	109.976(4)	
γ (°)	96.815(4)	
V ($Å^3$)	364.0(1)	1982(1)
Z	1	4
D (calc) (Mg/cm^3)	2.88	3.55
Temp. (K)	293	293
λ (Å)	0.71073	0.71073
Abs. coeff. (mm^{-1})	15.3	20.4
Obs. reflections ($F < 3\sigma$)	1913	2476
*wR*2	0.096	0.099
*R*1	0.052	0.073

blue crystals of $[Cu(en)_2][\{Cu_2Br_4\}]$ was obtained in approximately 40% yield based on Cu.

$[Cu(H_2NCH_2CH_2NH_2)_2][\{Cu_5Br_7\}]$, **2**. The hydrothermal reaction of $CuBr_2$ (0.670 g, 3 mmol), CuBr (0.430 g, 3.0 mmol), and ethylenediamine (0.20 mL, $d = 0.899\ g\,mL^{-1}$; 3.0 mmol) in 8 mL of H_2O in a mole ratio of 1 : 1 : 1 : 148 at 170°C for 3 days resulted in the formation of a single-phase product consisting of dark blue crystals of $[Cu(en)_2][\{Cu_5Br_7\}]$ (approximately 45% yield based on Cu).

CRYSTAL STRUCTURE DETERMINATION

Single-crystal diffraction data for **1** and **2** (Table 1) were measured at Syracuse University using a Siemens P4 diffractometer equipped with the SMART system (33) and using Mo$K\alpha$ radiation ($\lambda = 0.71073$ Å). Both data sets were corrected for Lorentz and polarization effects, and absorption corrections were made using SADABS (34). The structure solutions and refinements were carried out using SHELXL96 (35). Both structures were solved using direct methods and all of the nonhydrogen atoms were located from the initial solution or from subsequent electron density difference maps during the initial stages of the refinement. After all of the nonhydrogen atoms in each structure were located, the models were refined against F^2, first using isotropic and finally anisotropic thermal displacement parameters, until the final value of σ/Δ_{max} was less than 0.001.

TABLE 2
Atomic Coordinates and Isotropic Thermal Displacement Parameters ($Å^2$) for $[Cu(H_2NCH_2CH_2NH_2)_2][\{Cu_2Br_4\}]$ (1)

Atom	*x*	*y*	*z*	$U_{eq}{}^a$
Br(1)	0.5722(4)	0.0607(3)	0.0744(3)	0.034(1)
Br(2)	0.8422(3)	0.4405(3)	0.5881(3)	0.035(1)
Br(3)	0.2265(3)	0.0732(3)	0.4340(3)	0.033(1)
Br(4)	0.1883(3)	0.4259(2)	0.2259(3)	0.032(1)
Cu(1)	0.7065(8)	0.7504(6)	0.8304(6)	0.025(1)
Cu(2)	0.4718(6)	0.2508(5)	0.3277(5)	0.045(1)
Cu(3)	0.9409(7)	0.2543(5)	0.3299(5)	0.046(1)
N(1)	0.434(2)	0.558(2)	0.7624(2)	0.023(3)
N(2)	0.825(4)	0.689(3)	1.056(3)	0.043(6)
N(3)	0.988(4)	0.943(3)	0.900(3)	0.053(6)
N(4)	0.572(3)	0.812(3)	0.593(3)	0.027(4)
C(1)	0.473(6)	0.478(4)	0.904(4)	0.15(2)
C(2)	0.652(3)	0.583(3)	1.074(3)	0.055(7)
C(3)	0.925(2)	1.040(2)	0.763(2)	0.027(3)
C(4)	0.772(4)	0.909(2)	0.565(3)	0.050(6)

[a] Equivalent isotropic *U* defined as one-third of the trace of the orthogonalized U_{ij} tensor.

The positions of the hydrogen atoms were then calculated and fixed, and a final cycle of refinements was performed until σ/Δ_{max} was again less than 0.001.

RESULTS AND DISCUSSION

Structure of $[Cu(H_2NCH_2CH_2NH_2)_2][\{Cu_2Br_4\}]$

The atomic coordinates and isotropic thermal displacement parameters for $[Cu(en)_2][\{Cu_2Br_4\}]$ are listed in Table 2, while selected bond length and bond angle data are provided in Table 3. Figure 1 shows an ORTEP plot of the

TABLE 3
Selected Bond Lengths (Å) and Angles (°) for $[Cu(H_2NCH_2CH_2NH_2)_2][\{Cu_2Br_4\}]$

Cu(1)–N(2)	1.96(2)	Cu(2)–Br(4)	2.512(4)
Cu(1)–N(1)	1.99(2)	Cu(2)–Br(3)	2.536(5)
Cu(1)–N(3)	2.03(2)	Cu(3)–Br(1)	2.487(5)
Cu(1)–N(4)	2.05(2)	Cu(3)–Br(2)	2.494(4)
Cu(2)–Br(1)	2.485(4)	Cu(3)–Br(4)#2	2.505(5)
Cu(2)–Br(2)	2.499(5)	Cu(3)–Br(3)#2	2.562(5)
N(1)–Cu(1)–N(2)	83.3(8)	Br(2)–Cu(2)–Br(3)	113.7(2)
N(1)–Cu(1)–N(3)	179(1)	Br(2)–Cu(2)–Br(4)	114.5(2)
N(1)–Cu(1)–N(4)	95.0(7)	Br(3)–Cu(2)–Br(4)	94.0(3)
N(2)–Cu(1)–N(3)	96(1)	Br(1)–Cu(3)–Br(2)	104.9(2)
N(2)–Cu(1)–N(4)	178(1)	Br(1)–Cu(3)–Br(3)#2	113.2(2)
N(3)–Cu(1)–N(4)	85.4(8)	Br(1)–Cu(3)–Br(4)#2	115.1(2)
Br(1)–Cu(2)–Br(2)	104.9(2)	Br(2)–Cu(3)–Br(3)#2	114.4(2)
Br(1)–Cu(2)–Br(3)	114.3(2)	Br(2)–Cu(3)–Br(4)#2	115.8(2)
Br(1)–Cu(2)–Br(4)	115.7(2)	Br(3)–Cu(3)–Br(4)#2	93.6(2)

Note. Symmetry transformations used to generate equivalent atoms: (#1) $x - 1, y, z$; (#2) $x + 1, y, z$.

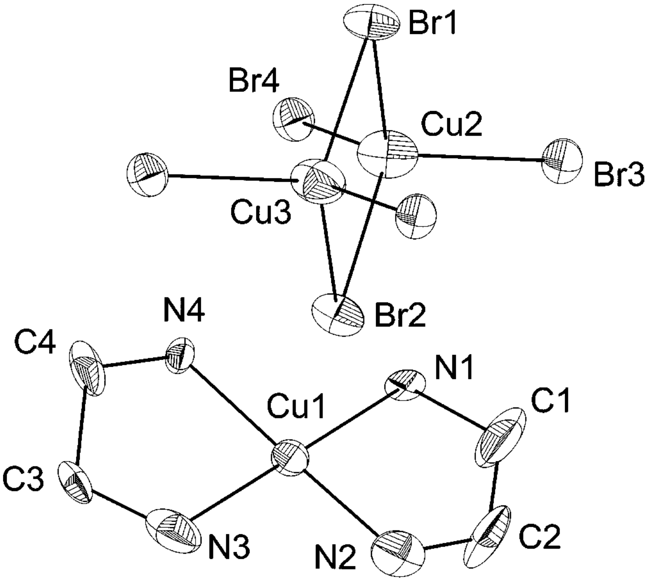

FIG. 1. An ORTEP plot showing the asymmetric unit and atom-labeling scheme for [Cu(H$_2$NCH$_2$CH$_2$NH$_2$)$_2$][{Cu$_2$Br$_4$}]. The hydrogen atoms are not shown.

coordination around the atoms of the asymmetric unit and provides the atom-labeling scheme for the structure [Cu(*en*)$_2$] [{Cu$_2$Br$_4$}]. [Cu(*en*)$_2$] [{Cu$_2$Br$_4$}] is structurally similar to the chloride [Cu(*en*)$_2$] [{Cu$_2$Cl$_4$}] (36) and the iodide [Cu(*en*)$_2$] [{Cu$_2$I$_4$}] (37). In this structure, which is shown in Fig. 2, the Cu(I) and halide ions form anionic one-dimensional [Cu$_2$Br$_4$]$^{2-}$ chains constructed from edge-sharing CuBr$_4$ tetrahedra and running parallel to the *a* axis. The divalent Cu(II) ions are each coordinated by two molecules of ethylenediamine to form [Cu(*en*)$_2$]$^{2+}$ units that occupy the interstices between the chains, providing charge balance for the structure. Long semicoordinate Cu(II)–Br bonds (~ 3.08 Å) result in a (4 + 2)-type coordination geometry around the Cu(II) ion and result in the cross-linking of adjacent [Cu$_2$Br$_4$]$^{2-}$ chains to form two-dimensional sheets (see Fig. 2).

The CuBr$_4$ tetrahedra are slightly distorted, with bond lengths ranging from 2.485(4) to 2.562(5) Å and with tetrahedral bond angles from 93.6(2)° to 115.8(2)°. The mean Cu(II)–N bond length (2.01(2) Å) and mean N–Cu–N angle of the bound *en* (84.4(8)°) found in the [Cu(*en*)$_2$]$^{2+}$ complex of the bromide are comparable to those found in the chloride (2.006(6) Å, 84.3(2)°) and iodide (2.01 Å, 85°). The observed thermal ellipsoids for some of the ligand atoms show large and asymmetric thermal parameters, particularly C(1), C(2), and N(3). This is due to a slight disorder in the position of the *en* ligands. Although it was possible to split the position for C(1), this did not result in a significant improvement in the refinement, and so it was described by a single position with a large thermal ellipsoid.

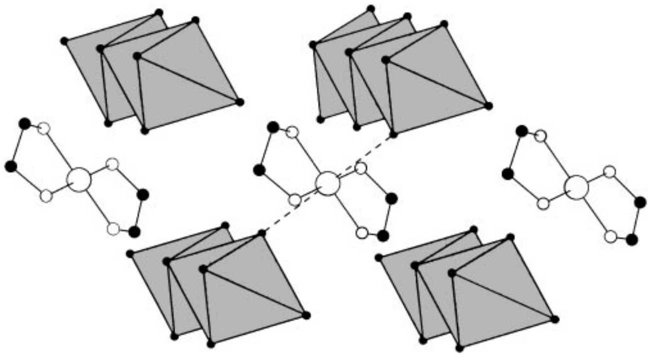

FIG. 2. A drawing of the [Cu(H$_2$NCH$_2$CH$_2$NH$_2$)$_2$] [{Cu$_2$Br$_4$}] structure. The Cu(II) atoms are shown as large open circles, while the nitrogen atoms are small open circles and the carbon atoms are black. The Cu$_2$Br$_4$ chains run parallel to the *a* axis. Adjacent chains are cross-linked by long semicoordinate bonds to the Cu(II) atom of the Cu(*en*)$_2$ units, shown as dashed lines, to form sheets of [Cu(H$_2$NCH$_2$CH$_2$NH$_2$)$_2$] [{Cu$_2$Br$_4$}].

Attempts to refine the structure of [Cu(*en*)$_2$][{Cu$_2$Br$_4$}] in the centrosymmetric space group $P\bar{1}$ were not satisfactory. The residual error for the centrosymmetric refinement was $wR2 = 0.123$, significantly higher than that obtained when the structure was determined in $P1$ ($wR2 = 0.096$). In addition, there were large distortions of the structural features, which indicated that $P\bar{1}$ was not the correct space group for the structural model. Among these were extreme distortions in the CuBr$_4$ tetrahedra, with Cu(I)–Br distances varying widely from 2.375(1) to 2.858(1) Å and tetrahedral Br–Cu(I)–Cr bond angles of 70.14(4)° to 131.43(4)°. In addition, the bonding features of the Cu(*en*)$_2$ complex were also

TABLE 4
Atomic Coordinates and Isotropic Thermal Displacement Parameters (Å^2) for [Cu(H$_2$NCH$_2$CH$_2$NH$_2$)$_2$] [{Cu$_5$Br$_7$}] (2)

Atom	*x*	*y*	*z*	U_{eq}[a]
Br(1)	0.1503(1)	$\frac{3}{4}$	0.1964(1)	0.0123(3)
Br(2)	0.4258(1)	$\frac{3}{4}$	− 0.0442(1)	0.0158(3)
Br(3)	0.3939(1)	0.6145(1)	0.2996(1)	0.0160(2)
Br(4)	0.1264(1)	0.5535(1)	0.4636(1)	0.0166(2)
Br(5)	0.2848(1)	$\frac{3}{4}$	0.6319(1)	0.0203(3)
Cu(1)	0	$\frac{1}{2}$	0	0.0119(3)
Cu(2a)	0.0420(3)	0.6771(2)	0.3773(4)	0.0266(8)
Cu(2b)	0.0051(3)	0.6510(2)	0.4050(4)	0.0287(8)
Cu(3)	0.2359(1)	0.6684(1)	0.4343(2)	0.0523(5)
Cu(4)	0.3503(1)	$\frac{3}{4}$	0.2176(2)	0.0189(4)
N(1)	0.0132(6)	0.4230(4)	0.1685(8)	0.018(2)
N(2)	− 0.1394(5)	0.4481(4)	− 0.0330(8)	0.015(2)
C(1)	− 0.0656(7)	0.3599(5)	0.1515(10)	0.018(2)
C(2)	− 0.1658(7)	0.4006(5)	0.0989(10)	0.016(2)

[a] Equivalent isotropic U defined as one-third of the trace of the orthogonalized U_{ij} tensor.

TABLE 5
Selected Bond Lengths (Å) and Angles (°) for $[Cu(H_2NCH_2CH_2NH_2)_2]\ [\{Cu_5Br_7\}]$ (2)

Cu(1)–N(2)	2.020(7)	Cu(2B)–Br(4)	2.326(3)
Cu(1)–N(2)#1	2.020(7)	Cu(3)–Br(1)	2.802(2)
Cu(1)–N(1)	2.021(7)	Cu(3)–Br(3)	2.548(2)
Cu(1)–N(1)#1	2.021(7)	Cu(3)–Br(4)	2.404(2)
Cu(2A)–Br(1)	2.489(4)	Cu(3)–Br(5)	2.358(2)
Cu(2A)–Br(2)#2	2.466(4)	Cu(4)–Br(1)	2.585(2)
Cu(2A)–Br(3)#2	2.716(4)	Cu(4)–Br(2)	2.590(2)
Cu(2A)–Br(4)	2.472(4)	Cu(4)–Br(3)	2.46(1)
Cu(2B)–Br(2)#2	2.331(4)	Cu(4)–Br(3)#3	2.46(1)
Cu(2B)–Br(3)#2	2.438(4)		
N(1)–Cu(1)–N(1)#1	180.0	Br(1)–Cu(3)–Br(3)	96.37(6)
N(1)–Cu(1)–N(2)	85.1(3)	Br(1)–Cu(3)–Br(4)	104.35(7)
N(1)–Cu(1)–N(2)#1	94.9(3)	Br(1)–Cu(3)–Br(5)	114.82(7)
N(1)#1–Cu(1)–N(2)	94.9(3)	Br(3)–Cu(3)–Br(4)	103.83(7)
N(1)#1–Cu(1)–N(2)#1	85.1(3)	Br(3)–Cu(3)–Br(5)	111.44(8)
N(2)–Cu(1)–N(2)#1	180.0	Br(4)–Cu(3)–Br(5)	122.43(7)
Br(1)–Cu(2A)–Br(2)#2	120.7(2)	Br(1)–Cu(4)–Br(2)	107.77(8)
Br(1)–Cu(2A)–Br(4)	112.29(13)	Br(1)–Cu(4)–Br(3)	104.55(5)
Br(2)#2–Cu(2A)–Br(4)	118.97(14)	Br(1)–Cu(4)–Br(3)#3	104.55(5)
Br(2)#2–Cu(2B)–Br(3)#2	110.07(13)	Br(2)–Cu(4)–Br(3)	101.37(5)
Br(2)#2–Cu(2B)–Br(4)	132.0(2)	Br(2)–Cu(4)–Br(3)#3	101.37(5)
Br(3)#2–Cu(2B)–Br(4)	113.35(14)	Br(3)–Cu(4)–Br(3)#3	135.10(9)

Note. Symmetry transformations used to generate equivalent atoms: (#1) $-x, -y+1, -z$; (#2) $x-\frac{1}{2}, y, -z+\frac{1}{2}$; (#3) $x, -y+\frac{3}{2}, z$.

distorted, with an N–Cu(II)–N bond angle of 75.5(2)° for the bound *en*, which is a much tighter bite angle for the ligand than the approximately 85° angle observed in the chloride and iodide compounds. Based on this evidence, we concluded that *P*1, with its better behaved structural model and lower residual error, represented the correct space group for the structure determination. It should be noted, however, that the Flack parameter indicated the presence of a chiral twin in the *P*1 model, with a refined phase fraction of 47(7)% of the enantiomorph reported here, the remainder being the inversion twin. Although *P*1 is an unusual space group choice, particularly as the iodide and chloride crystallize in centrosymmetric monoclinic space-groups, no higher metric symmetry could be determined for the unit-cell of the bromide, and no satisfactory model of the structure could be refined in the centrosymmetric $P\bar{1}$.

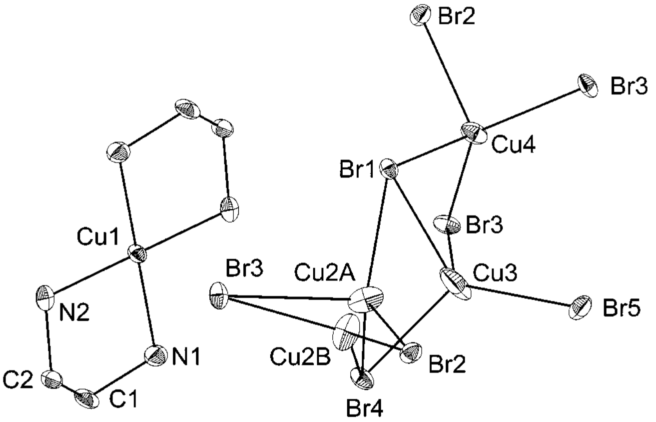

FIG. 3. An ORTEP plot showing the asymmetric unit and atom-labeling scheme for $[Cu(H_2NCH_2CH_2NH_2)_2][\{Cu_5Br_7\}]$. The hydrogen atoms are removed for clarity. Note how the bonding arrangement of the disordered Cu2 atom changes between tetrahedral for the Cu2A position to nearly trigonal planar at the Cu2B position.

Structure of $[Cu(H_2NCH_2CH_2NH_2)_2][\{Cu_5Br_7\}]$

The atomic coordinates and isotropic thermal displacement parameters for $[Cu(en)_2][\{Cu_5Br_7\}]$ are listed in Table 4, while selected bond length and bond angle data are provided in Table 5. An ORTEP plot of the asymmetric unit is shown in Fig. 3 and provides the atom-labeling scheme. The structure of this compound also contains edge-sharing $CuBr_4^-$ tetrahedra, which now form sinusoidal chains with the composition $[Cu_5Br_7]^{2-}$ (see Fig. 4). The chains of $[Cu_5Br_7]^-$ are cross-linked, by long (~ 2.99 Å) semicoordinate bonds to $Cu(en)_2$ units, in a manner similar to that observed in $[Cu(en)_2][\{Cu_2Br_4\}]$ and resulting in a three-dimensional network (see Fig. 5).

The structure of $[Cu(en)_2][\{Cu_5Br_7\}]$ is new, but the $[Cu_5Br_7]^{2-}$ chain bears structural similarities to the three-dimensional $[Cu_5Br_7]^{2-}$ framework of $(C_5H_5NH_2)Cu_5Br_7$ (38) and the $[Cu_5Br_7]^{2-}$ anions found in $[(NCH_3)(C_4H_9)_3]_2[Cu_5Br_7]$ (39). The underlying structural motif in all three compounds is the arrangement of the bromine atoms to form the vertices of a pentagonal bipyramid, a polyhedron that can also be visualized as the product of five face-sharing tetrahedra (see Fig. 6). In the discrete

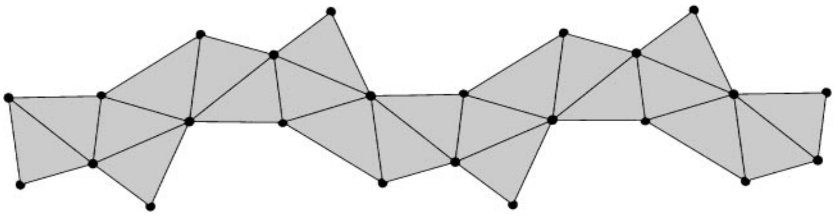

FIG. 4. A drawing of the sinusoidal $[Cu_5Br_7]^{2-}$ chain found in $[Cu(H_2NCH_2CH_2NH_2)_2][\{Cu_5Br_7\}]$. The chains run parallel to the *a* axis and are composed of edge-sharing $CuBr_4$ tetrahedra.

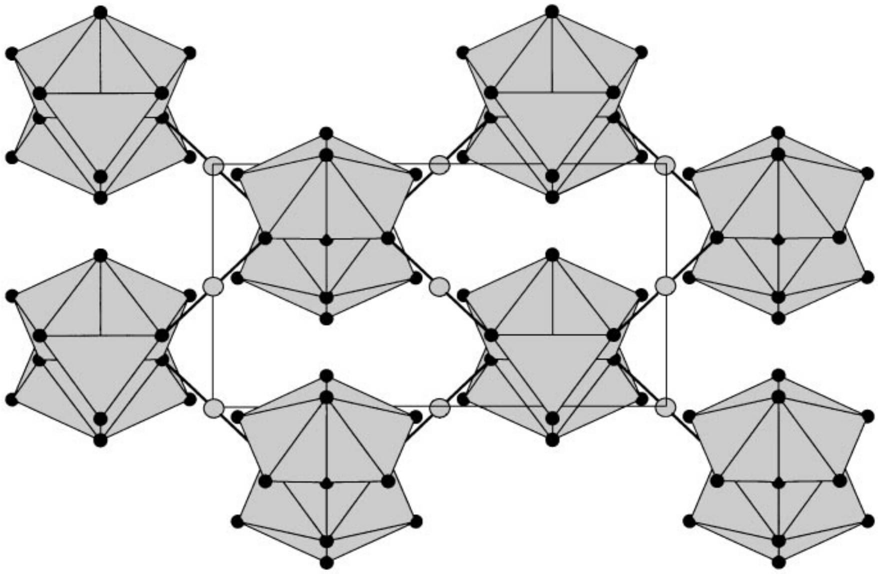

FIG. 5. A view of the $[Cu(H_2NCH_2CH_2NH_2)_2][\{Cu_5Br_7\}]$ structure down the [100] direction. The Cu(II) atoms are shown as gray spheres. The $[Cu_5Br_7]^{2-}$ chains are cross-linked by long semicoordinate bonds to the Cu(II) atom of the $Cu(en)_2$ units. Note that the ligands have been removed from the Cu(II) atom for clarity.

$[Cu_5Br_7]^{2-}$ ion reported by Andersson and Jagner, the five face-sharing tetrahedra each contain a copper atom. While the related iodide structure (40) shows only a small deviation from C_{5h} symmetry, the shorter Cu–Br bonds resulted in greater distortion of the face-sharing $CuBr_4$ tetrahedra. In the $[Cu_5Br_7]^{2-}$ chains found in $[Cu(en)_2][\{Cu_5Br_7\}]$ and in the three-dimensional $[Cu_5Br_7]^{2-}$ framework reported by Chan *et al.*, the bipyramids were connected by additional face-sharing tetrahedra formed by the bromine atoms of adjacent bipyramids (see Fig. 6). In the $(C_5H_5NH_2)Cu_5Br_7$ structure reported by Chan *et al.*, the 20 copper atoms of the unit cell are nonuniformly distributed among the 52 resulting tetrahedral sites, leading to only a partial occupancy of each tetrahedron. This minimizes the unfavorable arrangement caused by having adjacent occu-

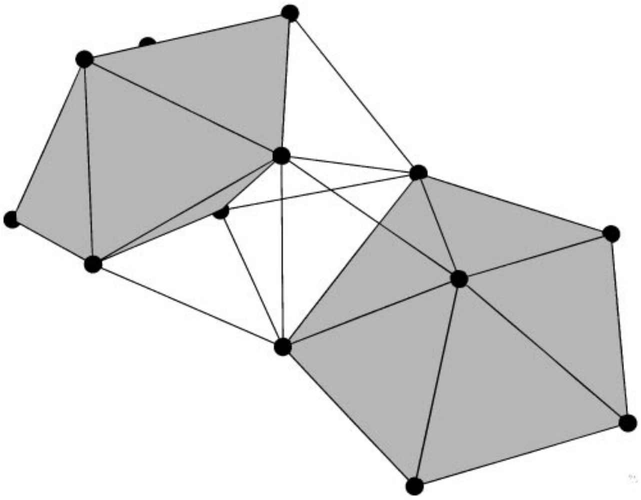

FIG. 6. A drawing of the pentagonal bipyramids formed by the bromine atoms in the $[Cu_5Br_7]^{2-}$ structures. The bipyramids can be described as five face-sharing tetrahedra as shown. It is possible to form a bridge of four additional face-sharing tetrahedra between two trigonal bipyramids as shown.

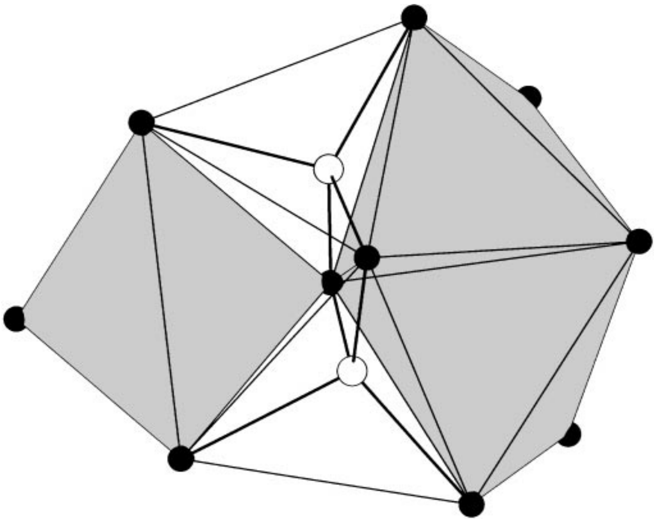

FIG. 7. The $[Cu_5Br_7]^{2-}$ structural subunit of the chains in $[Cu(H_2NCH_2CH_2NH_2)_2][\{Cu_5Br_7\}]$. The bromine atoms are represented by the small black spheres. Two of the five face-sharing tetrahedral sites of the pentagonal bipyramid are occupied by copper atoms, shown as open circles. The remaining three copper atoms occupy tetrahedral sites formed between neighboring pentagonal bipyramids, as illustrated in Fig. 6, and are represented by shaded tetrahedra.

pied face-sharing tetrahedra. In the $[Cu(en)_2][\{Cu_5Br_7\}]$ structure, the copper atoms are localized, with two atoms found within the tetrahedral sites of the pentagonal bipyramid, and the remaining three occupying inter-pyramidal, connective tetrahedral sites (see Fig. 7). The result in $[Cu(en)_2][\{Cu_5Br_7\}]$ is a chain of edge-sharing $CuBr_4$ tetrahedra, which removes the unfavorable condition of having face-sharing tetrahedra.

However, there are still significant distortions in the tetrahedra, the most notable being that formed by Cu(2) and the surrounding Br(1), Br(2), Br(3), and Br(4) atoms. This copper site is actually split into two positions. The position of Cu(2A) is tetrahedrally coordinated while that of Cu(2B) is in a slightly puckered trigonal coordination with Br(2), Br(3), and Br(4) (see Fig. 3). The shift from the A to the B position results in a shortening of the Cu(2)–Br(3) bond length from 2.716(4) to 2.438(4) Å. The anisotropic thermal ellipsoid of Cu(3) shows an elongation in the general direction of the long, 2.802(2) Å, Cu(3)–Br(1) bond, which may be indicative of a similar splitting in the Cu(3) position, although attempts to model this feature where unsuccessful. Similar distortions of the copper coordination toward a trigonal geometry were also observed by Andersson and Jagner in the discrete $[Cu_5Br_7]^{2-}$ ion. The distortion from tetrahedral to trigonal planar coordination is common in Cu(I) halides due to a second-order Jahn–Teller distortion in which the filled 3*d* orbitals mix.

ACKNOWLEDGMENT

All work at Syracuse University was funded by NSF Grant CHE 9617232. X-ray crystallographic data in CIF format are available from the author upon request.

REFERENCES

1. A. K. Cheetham, *Science* **264,** 794 (1994).
2. S. Mann, *J. Chem. Soc. Dalton Trans.* 3953 (1997).
3. S. Mann and G. A. Ozin, *Nature* (*London*) **382,** 313 (1996).
4. (a) J. V. Smith, *Chem. Rev.* **88,** 149 (1988). (b) M. L. Occelli and H. C. Robson, "Zeolite Syntheses." Am. Chem. Soc., Washington, DC, 1989.
5. C. T. Kresge, M. E. Leonowicz, W. J. Roth, J. C. Vartull, and J. S. Beck, *Nature* **359,** 710 (1992).
6. S. Mann, *Nature* **365,** 499 (1993).
7. R. C. Haushalter and L. A. Mundi, *Chem. Mater.* **4,** 31 (1992).
8. K. O. Kongshaug, H. Fjellvag, and K. P. Lillerud, *Chem. Mater.* **11,** 2872 (1999), and references therein.
9. P. Feng, X. Bu, and G. D. Stucky, *Nature* **388,** 735 (1997).
10. Z. Bircsak and W. T. A. Harrison, *Inorg. Chem.* **37,** 3204 (1998).
11. A. K. Cheetham, G. Ferey, and T. Loiseau, *Angew. Chem. Int. Ed.* **38,** 3268 (1999), and references therein.
12. V. Soghomonian, Q. Chen, R. C. Haushalter, J. Zubieta, and C. J. O'Connor, *Science* **259,** 1596 (1993).
13. M. I. Khan, L. M. Meyer, R. C. Haushalter, C. L. Schweitzer, J. .Zubieta, and J. L. Dye, *Chem. Mater.* **8,** 43 (1996).
14. D. Hagrman, J. Zubieta, D. J. Rose, J. Zubieta, and R. C. Haushalter, *Angew. Chem. Int. Ed. Engl.* **36,** 795 (1997).
15. P. J. Zapf, R. C. Haushalter, and J. Zubieta, *Chem. Mater.* **9,** 2019 (1997).
16. P. J. Zapf, C. J. Warren, R. C. Haushalter, and J. Zubieta, *Chem. Commun.* 1543 (1997).
17. D. Hagrman, R. C. Haushalter, and J. Zubieta, *Chem. Mater.* **10,** 361 (1998).
18. P. J. Zapf, R. P. Hammond, R. C. Haushalter, and J. Zubieta, *Chem. Mater.* **10,** 1366 (1998).
19. D. Hagrman, C. J. Warren, R. C. Haushalter, R. S. Rarig, Jr., K. M. Johnson, III, R. L. LaDuca, Jr., and J. Zubieta, *Inorg. Chem.* **37,** 3411 (1998).
20. D. Hagrman, P. J. Zapf, and J. Zubieta, *Chem. Commun.* 12830 (1998).
21. D. Hagrman, R. P. Hammond, R. C. Haushalter, and J. Zubieta, *Chem. Mater.* **10,** 3294 (1998).
22. D. Riori, O. Rouleau, L. Bouhedja, J. Livage, and G. Ferey, *Chem. Mater.* **12,** 67 (2000), and references therein.
23. P. J. Hagrman, D. Hagrman, and J. Zubieta, *Angew. Chem. Int. Ed.* **38,** 2638 (1999), and references therein.
24. P. Y. Zavalij and M. S. Whittingham, *Acta Crystallogr. B* **55,** 627 (1999), and references therein.
25. D. J. Chesnut, D. Hagrman, P. J. Zapf, R. P. Hammond, R. LaDuca, Jr., R. C. Haushalter, and J. Zubieta, *Coord. Chem. Rev.* **190–192,** 737 (1999), and references therein.
26. D. J. Chesnut, A. Kusnetzow, R. R. Birge, and J. Zubieta, *Inorg. Chem.* **38,** 2663 (1999), and references therein.
27. D. J. Chesnut, A. Kusnetzow, and J. Zubieta, *J. Chem. Soc. Dalton Trans.* 4081 (1998).
28. D. J. Chesnut and J. Zubieta, *Chem. Commun.* 1707 (1998).
29. C. R. Kagan, D. B. Mitzi, and C. D. Dimitrakopoulos, *Science* **286,** 945 (1999), and references therein.
30. J. D. Martin, A. M. Dattelbaum, T. A. Thornton, R. M. Sullivan, J. Yang, and M. T. Peachey, *Chem. Mater.* **10,** 2699 (1998), and references therein.
31. A. M. Dattelbaum and J. D. Martin, *Inorg. Chem.* **38** (1999) 6200.
32. J. R. D. DeBord, Y.-J. Lu, C. Warren, R. C. Haushalter, and J. A. Zubieta, *Chem. Commun.* 1365 (1997).
33. Siemens. "SMART Software Reference Manual." Siemens Analytical X-ray Instruments, Madison, WI, 1994.
34. G. M. Sheldrick, "SADABS: Program for Empirical Absorption Corrections," University of Gottingen, Germany, 1996.
35. G. M. Sheldrick, "SHELXL96. Program for the Refinement of Crystal Structures." University of Gottingen: Germany, 1996.
36. O. Simonsen and H. Toftlun, *Acta Crystallogr. C* **43,** 831 (1987).
37. B. Freckmann and K.-F. Tebbe, *Z. Naturforsch. B* **35,** 1319 (1980).
38. L. Y. Y. Chan, S. Geller, and P. M. Skarstad, *J. Solid State Chem.* **25,** 85 (1978).
39. S. Andersson and S. Jagner, *J. Crystallogr. Spectrosc. Res.* **18,** 591 (1988).
40. H. Hartl and F. Mahdjour-Abadi, *Angew. Chem. Int. Ed. Engl.* **23,** 378 (1984).
41. J. K. Burdett and O. Eisenstein, *Inorg. Chem.* **31,** 1758 (1992).